

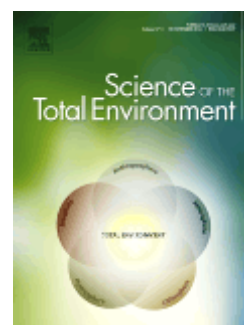
Accepted Manuscript

Using data from monitoring combined sewer overflows to assess, improve, and maintain combined sewer systems

To appear in: *Science of the Total Environment*

Received Date: 13 August 2014

Accepted: 25 October 2014



Elsevier Ltd.

DOI: 10.1016/j.envsci.2016.04.011

This is a PDF file of an unedited manuscript that has been accepted for publication. As a service to our customers we are providing this early version of the manuscript. The manuscript will undergo copyediting, typesetting, and review of the resulting proof before it is published in its final form. Please note that during the production process errors may be discovered which could affect the content, and all legal disclaimers that apply to the journal pertain.

© 2014. This manuscript version is made available under the CC-BY-NC-ND 4.0 license <http://creativecommons.org/licenses/by-nc-nd/4.0/>



1 **Using data from monitoring combined sewer overflows to assess, improve,**
2 **and maintain combined sewer systems**

3
4
5 A. Montserrat^{a,*}, Ll. Bosch^a, M.A. Kiser^a, M. Poch^{a,b}, Ll. Corominas^a
6
7

8 ^{a)} Catalan Institute for Water Research (ICRA), Scientific and Technological Park, H20 Building,
9 Emili Grahit 101,17003, Girona, Spain

10 ^{b)} Laboratory of Chemical and Environmental Engineering (LEQUIA), Universitat de Girona (UdG),
11 Campus de Montilivi, 17071, Girona, Spain
12
13

14 **Abstract**

15 Using low-cost sensors, data can be collected on the occurrence and duration of overflows in
16 each combined sewer overflow (CSO) structure in a combined sewer system (CSS). The
17 collection and analysis of real data can be used to assess, improve, and maintain CSSs in
18 order to reduce the number and impact of overflows. The objective of this study was to
19 develop a methodology to evaluate the performance of CSSs using low-cost monitoring. This
20 methodology includes (1) assessing the capacity of a CSS using overflow duration and rain
21 volume data, (2) characterizing the performance of CSO structures with statistics, (3)
22 evaluating the compliance of a CSS with government guidelines, and (4) generating decision
23 tree models to provide support to managers for making decisions about system maintenance.
24 The methodology is demonstrated with a case study of a CSS in La Garriga, Spain. The rain
25 volume *breaking point* from which CSO structures started to overflow ranged from 0.6 mm
26 to 2.8 mm. The structures with the best and worst performance in terms of overflow
27 (overflow probability, order, duration and CSO ranking) were characterized. Most of the
28 obtained decision trees to predict overflows from rain data had accuracies ranging from 70 to
29 83%. The results obtained from the proposed methodology can greatly support managers and
30 engineers dealing with real-world problems, improvements, and maintenance of CSSs.
31
32

33 **KEYWORDS**

34 CSO; CSS; wastewater; management; maintenance; performance; low-cost
35
36
37

1. INTRODUCTION

A combined sewer system (CSS) collects rainwater runoff, domestic sewage, and industrial wastewater in the same pipe. Normally, these systems will transport the total volume of sewage to a wastewater treatment plant (WWTP) for treatment. However, some rain episodes result in volumes of runoff that, when mixed with domestic and industrial waste, can exceed the capacities of a CSS. When capacity is exceeded, a combined sewer overflow (CSO) occurs, which is the discharge of untreated sewage (mixed with urban runoff) from a CSO structure directly into surface water.

Because CSOs contain untreated domestic and industrial waste, toxic materials, and debris, they impact the physicochemical, biological, hydraulic, and aesthetic status of receiving water bodies. For example, overflows can result in oxygen depletion, increased turbidity, and higher concentrations of micropollutants, heavy metals, and pathogenic and faecal organisms in surface waters (Passerat et al., 2011). Since the adoption of the Water Framework Directive 2000/60/EC by the European Union in the year 2000, Member States must apply local measures to address pollution affecting their surface waters. Most historic European cities, such as London, Paris and Rome, are drained by CSSs. In the United States, over 40 million people in 770 cities are served by CSSs, which release approximately 850 billion gallons of untreated wastewater and stormwater each year (EPA, 2004; EPA, 2014). Thus, decreasing the occurrence of overflows is an important part of reducing pollution in surface waters and requires accurate monitoring of CSO structures to provide reliable performance data to managers and engineers.

In previous studies, usually only a few CSO structures within a CSS were monitored (e.g. Gruber et al., 2005; Tetzlaff et al., 2005). Simultaneously monitoring all of the structures within one system would provide more useful information about the performance of the CSS as a whole but was until today cost prohibitive. Thus, researchers and engineers have resorted to using mathematical sewer models, calibrating the models with flow or level measurements taken in the sewer system (e.g. Kleidorfer et al., 2009; Gamerith et al., 2011). The main drawback of this modelling approach is that the real behavior of CSSs may not be accurately represented if the model was not calibrated properly. Schroeder et al. (2011) used real data to study the relationship between rainfall height and overflow activity, but the data was from only a few CSO structures within a network. More recently, Montserrat et al. (2013) developed and validated a low-cost method to measure the occurrence and duration of overflows using temperature sensors, which makes measuring all of the CSO structures within a CSS economically feasible.

Just as important as data collection, however, is the analysis and application of data. Municipalities, industries, and research centers regularly collect large amounts of data using the vast array of measurement technologies available today. The ability to analyze and learn from collections of data is essential to making informed decisions. Managers of CSSs must make important decisions concerning the maintenance and upgrade of CSO structures. The maintenance of sewer systems is a large cost to a municipality. For instance, the EPA estimated that for one CSO structure containing a screen facility, 10 overflows per year would have an annual operation and maintenance cost of approximately \$10,000 USD (EPA, 1993). With a 50-year lifespan, CSSs eventually need to be replaced or upgraded (Center for Sustainable Systems, 2013). In the United States, the upgrades could cost approximately \$64 billion USD over the next 20 years (EPA, 2008). Many municipalities cannot afford to pay for upgrades without federal and state aid, but federal spending on sewage infrastructure is falling (Tibbetts, 2005). Thus, municipalities or companies that manage sewers need to make

88 the best use of the money that is available to them for maintenance and upgrades.

89
90 If managers could monitor and analyze data on the occurrence and duration of overflows
91 within each and every CSO structure of a CSS, then they could assess how the structures
92 perform, pinpoint where the weak spots are within the system, and then make decisions
93 accordingly. The structures in which overflows occur most often are prime candidates for
94 maintenance and upgrades, and conversely, structures that have low frequencies of overflow
95 need less attention. Ideally, managers would have access to a tool that assesses or predicts
96 which structures are likely to overflow as a result of rain. Such a tool would help to
97 coordinate post-rainfall maintenance tasks, and costs could be decreased by spending less
98 time and effort checking on those structures that, through assessment, have been recognized
99 as unlikely to overflow. Similarly, managers could focus on updating only those structures
100 whose improvement would yield the greatest reduction of CSOs, which can best be
101 determined through monitoring and assessment. Using data from monitoring overflows can,
102 therefore, help CSS managers to decide on the most appropriate and cost-effective strategies
103 for maintenance and improvement, which is crucial when budgets for sewer infrastructures
104 are decreasing.

105
106 To the best of our knowledge, no prior studies have evaluated the performance of a CSS
107 based on data from monitoring the occurrence and duration of overflows in all or most of the
108 CSO structures within the system. The recent development of low-cost CSO-monitoring
109 methods (e.g. Montserrat et al., 2013) offers an excellent opportunity for the thorough
110 evaluation of CSSs. The insight gained from such an evaluation can be used to improve their
111 overall performance while reducing the negative impacts of overflows. The objective of this
112 study was to develop a methodology to evaluate the performance of CSSs using data from
113 low-cost monitoring. This methodology has four components: (1) assessing the capacity of a
114 CSS, (2) characterizing the performance of CSO structures, (3) evaluating the compliance of
115 a system with government guidelines, and (4) providing support for managers to make
116 decisions about system maintenance. The methodology is demonstrated with a case study of a
117 CSS in La Garriga, Spain.

118 119 120 **2. MATERIALS AND METHODS**

121 **2.1 Data collection**

122 We used a case study to demonstrate the methods described in this section, though they can
123 be applied to any CSS. The case study is in La Garriga, a village in the northeast of Spain.
124 This system collects urban and industrial wastewater from La Garriga, as well as a portion of
125 the wastewater from two adjacent municipalities. The drainage area of the whole urban
126 catchment is 370 Ha. The wastewater is conveyed to the La Garriga WWTP by gravity-
127 induced flow through 7.3-km-long circular pipes. Diameters of the pipes range from 300 to
128 800 mm. The CSS consists of a total number of 14 CSO structures, of which 8 are the side-
129 flow type and 6 are the transverse type. Structure 14 is located at the entrance of the WWTP.
130 A map of the system with the labeled CSO structures is illustrated in Fig. 1.

131
132 We monitored the occurrence and duration of CSOs in the La Garriga CSS over the course of
133 11 months (from July 2011 through May 2012). CSO Structures 1 through 14 were monitored
134 using low-cost temperature sensors, as described by Montserrat et al. (2013). Briefly, an
135 abrupt shift of temperature from a sensor installed at the overflowing structure indicates the
136 start of a CSO event, and the recovery of the signal back to the baseline temperature
137 corresponds to the end of the event. The data used in this study concerning the duration of the

138 CSO events and overflowing order for each structure, as well as the information on the rain
139 episodes, is provided in Supp. Data in the file 'Rain_CSO_Information.xlsx'. More
140 information about the materials and methods used to collect the data is given in Montserrat et
141 al. (2013). Of the 14 CSO structures that were monitored, we analyzed data from 12
142 structures; data from Structures 9 and 13 were not considered in the study due to the poor
143 quality (high background noise) of the gathered data.

144
145 During the evaluated period 53 independent rain episodes occurred and were monitored. The
146 inter-episode time between independent rain episodes was calculated as the average time the
147 system needs to return to dry weather flow conditions (6 hours in the La Garriga system).

148
149 (Figure 1)

150 151 **2.2 Methodology for CSS evaluation**

152 *2.2.1 Assessing the capacity of a CSS*

153 We assessed the capacity of a CSS by plotting the duration of overflows versus rain volume
154 for each rain episode and each individual structure. Fig. 2 shows two examples of how the
155 capacity of the CSS can be assessed by evaluating the behavior of individual structures using
156 overflow duration and rainfall data. The first example, Fig. 2A, belongs to a structure with
157 high activity in which overflows occur even with rain volumes as low as 2 mm. This example
158 indicates that the CSS does not have the capacity to assimilate the increased flow from rain
159 episodes. The second example, Fig. 2B, shows a CSS in which the structure starts to overflow
160 only after rainfall reaches a volume greater than 25 mm. In case A, data were fitted by a
161 linear curve (R^2 : 0.98), while data in case B were fitted better by a quadratic curve (R^2 : 0.95).
162 We also determined the *breaking point* of each CSO structure, defined as the rain volume at
163 which the structure starts to overflow, shown as dashed line in Fig. 2B. The lower the slope
164 and the greater the *breaking point*, the higher the capacity of the system or the better the
165 stormwater retention capacity of the catchment. These cases are examples of two extreme
166 scenarios and qualitatively show how CSS behavior changes as storage capacity increases.

167
168 Figs. 2A and 2B were generated using a numerical model example of a subcatchment of the
169 case study, and afterwards the methodology was applied to the collected field data. The
170 model was developed using the Storm Water Management Model version 5.0.022
171 (Rossmann, 2007), and details about the model development and the making of the CSO
172 duration-rain volume curves are provided in Supp. Data.

173
174 (Figure 2)

2.2.2 Characterizing the performance of CSO structures

We developed a detailed statistical analysis on the data we collected of the occurrence and duration of CSO events. To characterize system performance, we calculated and plotted the following parameters for each CSO in the network over the entire data collection period: (i) total number of overflows, (ii) total duration of overflows (sum of the durations of all overflows in the period), (iii) average overflow duration, (iv) the average chronological order that a CSO structure begins to overflow compared to all the other structures in the network, and (v) overflow probability. These parameters are indicators of the performance of each CSO structure and can be used to compare different structures within the same system. To calculate the total number of overflows, we counted any number of overflows that occurred during one independent rain episode as a single, independent CSO event. 53 independent rain episodes occurred during the study period, so the maximum number of CSO events per structure would be 53 for this case-study.

We developed ranking curves to provide information about the order in which a structure overflows with respect to the other structures in a CSS. For each rain episode, we identified which structure overflowed first and assigned a value of 1 as its overflow position; then we assigned consecutive values of overflow positions to the other structures in the order that they overflowed. For a particular structure (z) and for each overflow position (i), we used Eq. (1) to calculate the *CSO ranking index* – the fraction of CSO events in which the structure overflowed in position i or lower.

$$CSORanking_{(z,n)} = \frac{\sum_{i=1}^n C_{i,z}}{\#_z} \quad \text{Eq. (1)}$$

where $\#_z$ is the total number of times during the monitored period that z overflowed, $C_{i,z}$ is the number of times that z overflowed in i^{th} position, and n is the number of CSO structures in the CSS. The maximum value of i is equal to n .

The ranking curves are obtained by plotting the ranking index of each CSO structure with respect to overflow position i and reach a maximum y-axis value of 1. To compare the performance of different structures, each curve was fitted by a power function ($F(x)=X^b$), and the exponent b of the function was used to rank the structures according to their ranking index.

Confidence intervals were calculated to see whether significant statistical differences existed among the parameter values of the different CSO structures. The confidence interval (Ci) (Eq. (2)) gives the range of values in which the true average is located.

$$Ci = Avg \pm E \frac{SD}{\sqrt{n}} \quad \text{Eq. (2)}$$

where Avg is the average value of the sample, SD is the standard deviation of the sample, n is the number of samples, and E is a statistical value that depends on the size of the sample and the confidence limits. The value for E is found in the *T-table* (for $n < 25$) or *Z-table* (for $n \geq 25$). The Ci with 95% confidence limits was calculated for each parameter. In the case of parameters that represent proportions, the Ci_p was calculated as

$$Ci_p = p \pm E \frac{\sqrt{p(1-p)}}{\sqrt{n}} \quad \text{Eq. (3)}$$

where p is the proportion of the studied variable.

The confidence interval Ci was calculated for the variables *average overflow duration* and *average chronological order*, while the Ci_p was calculated for the *overflow probability*. The calculated confidence intervals are valid for normally distributed variables, such as those calculated here, since they represent averages or proportions over a sample of data from each variable.

2.2.3 Evaluating the compliance of a CSS with government guidelines

The number of overflows per year per CSO structure is a common emission standard referred to in CSO regulation guidelines. Hence, we can evaluate the compliance of a CSS with government guidelines by comparing the number of overflows measured in each CSO structure of a CSS to the maximum number of overflows suggested by the guidelines. Table 1 gives some examples of the permitted number of overflows per year in six countries. In some cases, such as in Belgium, Denmark, or the Netherlands, the permitted number of overflows is dependent on the sensitivity of the receiving waters (Zabel et al., 2001). Sometimes, the threshold is estimated using models fed with representative pluviometric data of the region (e.g. the ITOGH in Spain described in Hernandez et al., 2011). It is worth noting that the guidelines are site-dependent and differ in the permitted number of overflows. Furthermore, the definition of overflow frequency is crucial. For instance, overflows can be counted as events (or spills), or as overflow days (which can be calendar days or running days). Taking one definition or another significantly changes the results (Dirckx et al., 2014).

(Table 1)

2.2.4 Providing support to managers for CSS maintenance

Decision trees are predictive models based on supervised machine learning. In supervised learning, a teacher (the user) gives a computer program example input data and their desired or known outputs, and the program learns a general rule that maps inputs to outputs. The map is known as a decision tree, which can then be used to predict the results of input data with unknown outputs. If trained on high-quality data, decision trees can make accurate predictions (Kingsford and Salzberg, 2008). The output of decision trees visually and explicitly represent predictions and can therefore be an important tool for decision making.

Because of their power and utility for aggregating diverse types of data and making predictions, decision trees have become very popular in a variety of fields, such as environmental engineering, medicine, and bioinformatics (Kingsford and Salzberg, 2008; Rudin, 2012). In the field of wastewater treatment, decision trees have been used to design and develop tools to cope with highly complex environmental problems such as wastewater plant supervision or the selection of wastewater treatment systems (Poch et al., 2004), aimed at assisting in the decision-making process to find an optimal solution.

276 In this study, we constructed decision trees for CSO structures as part of a tool to help
277 managers make decisions about CSS maintenance. A decision tree consists of nodes
278 connected by branches. There are two types of nodes in a decision tree: (1) internal nodes that
279 represent explanatory variables, and (2) terminal nodes, or leaves, which give the response
280 variable. Branches extend from internal nodes, with each branch defining a range of values
281 for the internal node. The appropriate branch will be selected depending on the value for the
282 internal node input by the user, leading to the next node. The process of branch selection
283 continues until a prediction (leaf) is reached.

284
285 The specific technique used to induce the decision trees was the *J48 algorithm*, which is
286 based on the *C4.5 algorithm* (Quinlan, 1993). Waikato Environment for Knowledge Analysis
287 (WEKA) Version 3.6.0 was used to generate the trees. The input data, or explanatory
288 variables, were rain characteristics (total volume, duration, maximum intensity, and time
289 since the previous rain episode), and the output, or response variable, was whether or not the
290 CSO structure overflowed. Data on rain episodes and CSO occurrence and duration were
291 used to build each decision tree through a *k-fold* cross-validation procedure; the data set is
292 randomly split into more or less equal *k* folds (or subsets), and the algorithm is run *k* times.
293 At each time, *k-1* folds are used as training data to generate the tree, while the remaining fold
294 is used as validation data. The prediction error (i.e. the accuracy) of the trees is calculated
295 from the validation data. A thorough description of the cross-validation procedure is given in
296 Rokach and Maimon (2008). This technique is especially suited for relatively small data sets
297 ($n < 1000$; De'ath, 2007), since the trees are trained on all the data sets. In this study, $k=10$
298 folds was used. Furthermore, we developed a user-friendly computer application to visualize
299 the different decision trees that are obtained with known characteristics of a rain episode. The
300 application was programmed in JScript and is available in Supp. Data in the
301 'CSO_application' zip file.

302 303 304 **3. RESULTS AND DISCUSSION**

305 **3.1 Assessing the capacity of a CSS**

306 For each of the 12 structures evaluated, we plotted the CSO duration versus rain volume for
307 each rain episode during the 11-month study period. The rain episodes ranged in volume from
308 0.4 to 51.4 mm. Fig. 3 illustrates two examples with different behaviour obtained from the
309 collected data. Fig. 3A refers to Structure 11 and shows that for rain volumes lower than 20
310 mm only a few overflow events occurred, with durations between 6-27 min. Even for rain
311 volumes larger than 20 mm all but one of the overflow durations were less than 50 min. In
312 this case, the rain volume *breaking point* at which the structure starts to overflow was
313 established at 2.2 mm. For that case, non-linearity holds between the rain volume and the
314 overflow duration (R^2 : 0.31). Fig. 3B corresponds to Structure 7, for which the *breaking point*
315 of the system was also set at 2.2 mm. However, after a rain volume of 15 mm, increasing rain
316 volumes resulted in longer CSO durations, reaching saturation around 200 min. The data
317 were fitted by a sigmoidal curve (R^2 : 0.86). The rain volume *breaking points* for the other
318 structures ranged from 0.6 mm to 2.8 mm (provided in Supp. Data).

319
320
321 (Figure 3)
322
323

324 Plotting overflow duration versus rainfall volume and fitting the data is useful to assess the
325 behavior of each CSO structure and evaluate the efficacy of the CSS's design. CSSs are
326 typically designed with a target value for the capacity of the system, for instance two times
327 the mean dry weather flow (De Toffol, 2006). Whether or not the target capacity is achieved
328 by the CSS can be determined from collecting and analyzing data as described here.

329

330

331 **3.2 Characterizing the performance of CSO structures**

332 By applying our characterization method to the case study, we were able to gain an
333 understanding of the performance of each CSO structure in the La Garriga CSS and highlight
334 the system's weak points. Structures 7 and 14 each had the greatest numbers of overflow
335 events, 36 and 49 respectively, during the 11-month study period. By far, Structure 14 (at the
336 inlet of the WWTP) had the greatest total overflow duration, with close to 10,000 minutes
337 (about 7 days) for the 53 rain episodes (see Supplementary Data, Fig. SD2). The other CSO
338 structures had total overflow durations ranging from 294 to 2,113 minutes.

339

340 Fig. 4 shows the averages of the variables that we evaluated with a 95% *Ci*. For *overflow*
341 *probability*, Structure 14 had a probability of overflowing (avg = 0.9) during any given rain
342 episode that was significantly greater than the probabilities of all the other CSO structures.
343 Structure 7 had the second highest average overflow probability (avg = 0.7), but not
344 significantly different than other structures. Structure 11 had the lowest probability (avg =
345 0.3). As for *average overflow duration*, Structure 14 had a significantly higher value (avg =
346 186 min) than the other structures, and Structure 11 had the lowest overflow duration on
347 average (5.5 min). The overflow durations of the other structures in the network were
348 between 10 and 40 minutes, with no significant difference among them. Finally, analysis of
349 the *average order of overflow* showed that Structure 7 tended to overflow first (average order
350 of overflow = 2.6), with a significant difference between the order of overflow of most of the
351 other structures. Structure 10 had the second average value for overflow order (avg = 3.1),
352 and Structures 1, 11, and 12 tended to overflow last (averages around 7).

353

354 The inclusion of the *Ci* in the average allows us to state with 95% confidence whether or not
355 there is significant difference among the evaluated variables of the different CSO structures.
356 In addition to the obvious importance of Structures 14 and 7 for the performance of this CSS,
357 comparisons can be made between select groups of structures in order to find significant
358 differences between them. For instance, Structures 2 and 11 had on average less *overflow*
359 *duration* than Structures 5 and 7, and Structures 7 and 10 overflowed on average before
360 Structures 1, 5, 6, 11, and 12.

361

362 (Figure 4)

363

364 Each CSO structure can be characterized by a *ranking index*, based on the orders in which a
365 structure overflows during rain episodes. Fig. 5 shows the *ranking* curves for each CSO
366 structure and its corresponding exponent *b*. The vertical axis of the plot is the ranking index
367 and the horizontal axis is the i^{th} place of overflow in the network. For example, in the case of
368 Structure 7, almost 80% of the times that it overflowed, it was in the first 3 places (1st, 2nd, or
369 3rd structure in the network to overflow). Structure 10 had a similarly high ranking. On the
370 other hand, Structure 11 overflowed in the first three places only around 7% of the times that
371 it overflowed. Looking at the ranking curves, Structures 7 and 10 had curves with the lowest
372 value for exponent *b* (0.26 and 0.31, respectively), while Structures 1 and 11 had the highest
373 exponents (1.3 for each). Structures 7 and 10 overflowed in the first 4 places around 80 to

374 85% of the time – more than any other structures, and Structures 1 and 11 overflowed in the
375 first 4 places the least – approximately 20% of the time. The lower the value of b , the sooner
376 the structure is likely to overflow within the network.

377
378 (Figure 5)

379
380 Using these methods for characterizing system performance, Structures 14, 7, and 10 stand
381 out as problematic, at least compared to the other structures. Characterization of the structures
382 highlighted those with the best and worst performance in terms of overflow. It should be
383 noted that for a CSO structure that overflows often, the problem may not be with the structure
384 itself but may originate from other, more distant factors, such as the overloading conditions
385 downstream from the system. A proper investigation must be carried out to determine the true
386 cause of frequent overflows. Nonetheless, from the characterization information,
387 management strategies can be devised and implemented, such as seeking out the cause of
388 overflows or installing upgrades or extra reinforcements. Without this analysis, it would not
389 have been possible to know which of the CSO structures were most reactive to rain episodes.

390
391

392 **3.3 Evaluating the compliance of the CSS with government guidelines**

393 Fig. 6 is a schematic of the CSS of La Garriga and includes the number of CSOs measured
394 during the 11-month study for each CSO structure. We compared the number of overflows
395 for each CSO structure in the La Garriga CSS during the study period to the number of
396 overflows per CSO structure per year permitted by Spain's ITOHG, which is 15-20
397 overflows. We are aware of the specificity of ITOHG to the Galician region with a very
398 particular pluviometric regime. Hence, the results obtained here are for illustration purposes
399 only. The 11 months of study accumulated a rainfall volume of 525 mm. The analysis of the
400 rainfall series from 2009 to 2013 registered in the La Garriga rain gauge resulted in an
401 average annual precipitation of 642 mm. Considering a 95% confidence interval, the
402 precipitation of the evaluated period was assumed to be representative of an average
403 pluviometric year. Our study period was only 11 months, and we recognize that a 12-month
404 study period would have been best for comparison with government guidelines for annual
405 overflows. Most of the structures in our 11-month case study exceeded the number of
406 recommended overflows per year. Only three out of the 12 CSO structures (Nos. 2, 11, and
407 12) in the La Garriga CSS meet or closely meet the ITOHG guidelines. None of the CSO
408 structures in La Garriga would comply with the CSO guidelines of the countries outside of
409 Spain shown in Table 1.

410

411 The CSO structures with the least overflows were CSO 2, 11, and 12 (≤ 21 overflows). CSO
412 2 is a lateral structure that receives discharges from a residential neighborhood with a highly
413 pervious surface. CSOs 11 and 12 are located at the beginning of the system. Moving further
414 down the system, the number of overflows is higher. CSO 5 (30 overflows) and 7 (36
415 overflows) are lateral structures located at the outlet of densely urban areas. CSO 4 (29
416 overflows) is located along the main sewer trunk and receives most of the runoff from La
417 Garriga and contributing areas (all the urban and part of the industrial areas). CSO 3 (32
418 overflows) is a lateral structure at the outlet of a recently developed industrial area with a
419 mostly impervious surface. CSO 1 (29 overflows) is a lateral structure that receives
420 wastewater from part of a neighboring municipality. Given that CSO 1 is located towards the
421 end of the system, backwater effects could be increasing the number of overflows at this
422 point. At the very end of the system and at the entrance of the WWTP is CSO 14, which had
423 by far the highest number of overflows (49) of all the CSO structures.

424
425 Evaluating the compliance of a CSS with government guidelines can help to define
426 appropriate CSS management strategies, which can range from upgrades to improve CSS
427 performance, to measures aimed at increasing the stormwater retention capacity of the
428 catchment, so that local overflow recommendations are met. However, as addressed in
429 section 2.2.3, compliance with standards is a major issue in which site-specific regulations
430 have to be considered.

431
432 (Figure 6)

433
434

435 **3.4 Providing support to managers for CSS maintenance**

436 For our case study of the La Garriga CSS, we constructed a decision tree for each CSO
437 structure. Supp. Data Table SD2 gives a summary of the configurations and accuracies of the
438 decision trees constructed for the La Garriga CSS. Overall, the trees had simple
439 configurations. The number and types of explanatory variables needed to make predictions
440 differ among the CSO structures. In other words, different rain characteristics will cause
441 different structures to overflow more than others. For instance, Structures 3, 7, 8, and 10 need
442 only one explanatory variable to reach the response variable. Rain volume will be the primary
443 determinant of whether or not Structures 3 and 7 overflow, while the maximum intensity of a
444 rain episode will mainly control whether or not Structures 8 and 10 overflow. The more
445 complex a tree is, the more explanatory variables are involved. An exception was the tree for
446 Structure 7, which had 8 branches, 4 nodes, 5 leaves, and only one explanatory variable (rain
447 volume). As an example, a description of the decision tree made for Structure 14 is included
448 in Supp. Data, Fig. SD3. Structure 14 had the highest accuracy (91%) and Structure 2 the
449 lowest (57%). The accuracy of the other trees ranged between 70 and 83%.

450
451 Fig. 7 shows both the successful and the incorrect overflow predictions made by the model
452 for each CSO structure during 53 rain episodes. In this example, the trees predicted whether
453 or not a CSO structure would overflow with given rain volumes of each rain episode, which
454 were sorted from highest to lowest rain volume along the x -axis. The white spaces in the
455 figure denote correct predictions of structures that did not overflow during a particular rain
456 episode, while the black spaces represent correct predictions of the occurrence of overflow.
457 Grey squares show where the model's predictions did not match observations (real data from
458 monitored CSOs). For all the rain episodes and structures, the prediction succeeded in 89% of
459 cases.

460
461 (Figure 7)

462

463 We developed a computer application, called “La Garriga CSO Network Simulator”, to
464 visualize the different decision trees that are obtained with known characteristics of a rain
465 episode. The application has a user-friendly interface that allows predictions to easily be
466 made and clearly understood for the La Garriga CSS. Though this particular application was
467 made for the La Garriga CSS, the same application format can be developed for any CSS and
468 used by managers, engineers, or maintenance crew. For a description of the interface and to
469 open the application, see the ‘CSO_application’ zip file in Supp. Data.

470

471 Typically, sewer maintenance crew have to visit each CSO structure in a CSS after rainfall to
472 check if overflow occurred and to do any maintenance work that might be necessary.
473 Structures that don't overflow usually would not require checking or maintenance post-

474 rainfall. Maintenance time, and therefore money, would be better spent by focusing on the
475 structures that have a tendency to overflow. Thus, the CSO prediction tool described here
476 could save time and money for sewer managers and crew by indicating the CSO structures
477 that need to be checked after a rain episode with given characteristics. This is especially true
478 for large CSSs with high numbers of CSO structures, when one sewer management company
479 must manage several CSSs in one or more municipalities, or when maintenance crew is
480 limited. The prediction of overflows through decision trees would also present an advantage
481 for real-time control of CSSs. By means of weather forecast information (rain volume,
482 duration and max. intensity), it would be possible to identify which structures overflow and
483 take actions to maximize the usage of CSS volume (Schütze et al., 2004).

487 **4. CONCLUSIONS**

488 In order to assess, improve, and maintain CSSs, we developed a comprehensive methodology
489 to analyze data collected from the low-cost monitoring of CSO structures. Monitoring was in
490 the form of measuring rainfall data and the occurrence and duration of CSOs using
491 temperature sensors.

492
493 CSS capacity is assessed by analyzing the relationship between the overflow duration and
494 rain volume for each single CSO structure and each rain episode. In the case study, the La
495 Garriga CSS was found to have a capacity in which overflows occur with rain volumes as
496 little as 2 mm. To characterize the performance of each structure within a CSS, a statistical
497 analysis is used. Through the statistical analysis, we determined the overflow probability and
498 ranking index of each structure in the La Garriga CSS, which highlighted the structures that
499 were most problematic. To evaluate compliance with legislation, the measured number of
500 overflows for each CSO structure was compared to the annual permitted number of overflows
501 per structure recommended by government-issued guidelines. Finally, to predict which
502 structures in a CSS will overflow after a rain episode, we constructed a predictive model
503 using decision trees, which can be used to optimize post-rainfall maintenance of CSSs. The
504 decision trees for the La Garriga CSS had accuracies ranging from 70 to 83%, with two
505 exceptions – one tree with an accuracy of 91% and another with 57%.

506
507 The methodology presented in this study is an effective and affordable package for
508 municipalities and companies that manage sewer systems, as well as for engineers and
509 scientists who need to gain a better understanding of the CSSs they are providing services for
510 or in which they are conducting studies. Each of the analyses included in the methodology is
511 based on the direct, simultaneous measurements of overflows in all of the CSO structures
512 within a CSS. In this study, data was collected from sensors by manually downloading the
513 data onto a computer once per month. To make CSO monitoring even more efficient and
514 effective, future studies should use online sensors that collect and transmit data to online data
515 storage in real time. A program could be set up to analyze the raw data as it is transmitted.
516 Real-time data collection and analysis would negate the need for predictive models and could
517 further reduce maintenance costs. Online sensors are the future of monitoring and are
518 recommended for municipalities that can afford to install them.

522 **5. ACKNOWLEDGMENTS**

523 The authors would like to thank the Consorci per la Defensa de la Conca del Riu Besòs, in
524 particular the Drenatges Urbans del Besòs. Support for this project was provided by the
525 ENDERUS Project (CTM-2009-13018) and the predoctoral grant FPI BES-2010-039247,
526 founded by the Spanish Ministry of Science and Innovation. Lluís Corominas received the
527 postdoctoral Juan de la Cierva grant (JCI-2009-05604) from the Government of Spain and the
528 Career Integration Grant (PCIG9-GA-2011-293535) from the EU. The authors also
529 acknowledge the support from the Economy and Knowledge Department of the Catalan
530 Government through the Consolidated Research Group (2014 SGR 291) – Catalan Institute
531 for Water Research. Finally, we would like to thank Prof. Dirk Muschalla for his suggestions
532 during the interpretation of the data.

533
534
535
536 **6. REFERENCES**

537
538 Center for Sustainable Systems. U.S. Wastewater Treatment Fact sheet. University of
539 Michigan; 2013 [Pub. No. CSS04-14].

540
541 De'ath G. Boosted trees for ecological modelling and prediction. *Ecology* 2007;88(1):243-51.

542
543 De Toffol S. Sewer system performance assessment – an indicators based methodology. PhD
544 Thesis in Unit of Environmental Engineering, University of Innsbruck (2006).

545
546 Dirckx G, Vinck E., Weemaes M, Hellinck N. Operational optimization potential of storage
547 (sedimentation) tanks based on long-term continuous water level monitoring. Proceedings of
548 the IWA World Water Congress & Exhibition; 2014, Lisbon, Portugal.

549
550 EPA. Manual on Combined Sewer Overflow Control. U.S. Environmental Protection
551 Agency; 1993 [EPA625-R-93-007].

552
553 EPA. Report to Congress – Impacts and Control of CSOs and SSOs. U.S. Environmental
554 Protection Agency; 2004 [EPA833-R-04-001].

555
556 EPA. Reducing Stormwater Costs through Low Impact Development (LID) Strategies and
557 Practices. U.S. Environmental Protection Agency; 2007 [EPA841-F-07-006].

558
559 EPA. Clean Watershed Needs Survey 2008: Report to Congress. U.S. Environmental
560 Protection Agency; 2008 [EPA 832-R-10-002].

561
562 EPA. CADDIS Volume 2: Sources, Stressors & Responses,
563 http://www.epa.gov/caddis/ssr_urb_ww2.html; 2014. [date accessed: 15/07/2014].

564
565 FWR. Urban Pollution Management Manual. 3rd ed. Marlow: Foundation for Water
566 Research; 2012.

567
568 Gamerith V, Gruber G, Muschalla D. Single- and Multievent Optimization in Combined
569 Sewer Flow and Water Quality Model Calibration. *Journal of Environmental Engineering*
570 2011;137(7):551-58.

572 Gruber G, Winkler S, Pressl A. Continuous monitoring in sewer networks an approach for
573 quantification of pollution loads from CSOs into surface water bodies. *Water Sci Technol*
574 2005;52(12):215-23.

575

576 Hernáez D, Blanco JP, Arias R, Sánchez EM, Suárez J, Puertas J, et al. ITOHG: CSO
577 regulations in NW Spain. Proceedings of the 12th International Conference on Urban
578 Drainage; 2011, Porto Alegre, Brazil.

579

580 Kingsford C, Salzberg SL. What are decision trees?. *Nat Biotechnol* 2008;26(9):1011-13.

581

582 Kleidorfer M, Möderl M, Fach S, Rauch W. Optimization of measurement campaigns for
583 calibration of a conceptual sewer model. *Water Sci Technol* 2009;59(8):1523-30.

584

585

586 Montserrat A, Gutierrez O, Poch M, Corominas Ll. Field validation of a new low-cost
587 method for determining occurrence and duration of combined sewer overflows. *Sci Total*
588 *Environ* 2013;463-464:904-12.

589

590 Passerat J, Ouattara NK, Mouchel J-M, Rocher V. Impact of an intense combined sewer
591 overflow event on the microbiological water quality of the Seine River. *Water Res*
592 2011;45:893-903.

593

594 Poch M, Comas J, Rodríguez-Roda I, Sánchez-Marré M, Cortés U. Designing and building
595 real environmental decision support systems. *Environmental Modelling & Software*
596 2004;19:857-73.

597

598 Quinlan JR. *C4.5: Programs for Machine Learning*. San Mateo: Morgan Kaufmann
599 Publishers; 1993.

600

601 Rokach L, Maimon O. *Data Mining with Decision Trees – Theory and Applications*.
602 Singapore: World Scientific Publishing Company; 2008.

603

604 Rossmann LA. *Storm water management model user’s manual, version 5.0*. Cincinnati: U.S.
605 Environmental Protection Agency; 2007.

606

607 Rudin C. *Prediction: Machine Learning and Statistics - MIT Course N° 15097*,
608 [http://ocw.mit.edu/courses/sloan-school-of-management/15-097-prediction-machine-](http://ocw.mit.edu/courses/sloan-school-of-management/15-097-prediction-machine-learning-and-statistics-spring-2012/)
609 [learning-and-statistics-spring-2012](http://ocw.mit.edu/courses/sloan-school-of-management/15-097-prediction-machine-learning-and-statistics-spring-2012/); 2012. [date accessed: 05/08/2014].

610

611 Schroeder K, Riechel M, Matzinger A, Rouault P, Sonnenberg H, Pawlowsky-Reusing E, et
612 al. Evaluation of effectiveness of combined sewer overflow control measures by operational
613 data. *Water Sci Technol* 2011;63(2):325-30.

614

615 Schütze M, Campisano A, Colas H, Schilling W, Vanrolleghem PA. Real time control of
616 urban wastewater systems-where do we stand today?. *Journal of Hydrology* 2004;299:335-
617 48.

618

619 Tetzlaff D, Uhlenbrook S, Grottker M, Leibundgut CH. Hydrological assessment of flow
620 dynamic changes by storm sewer overflows and combined sewer overflows on an event-scale
621 in an urban river. *Urban Water Journal* 2005;2(4):201-14.

622

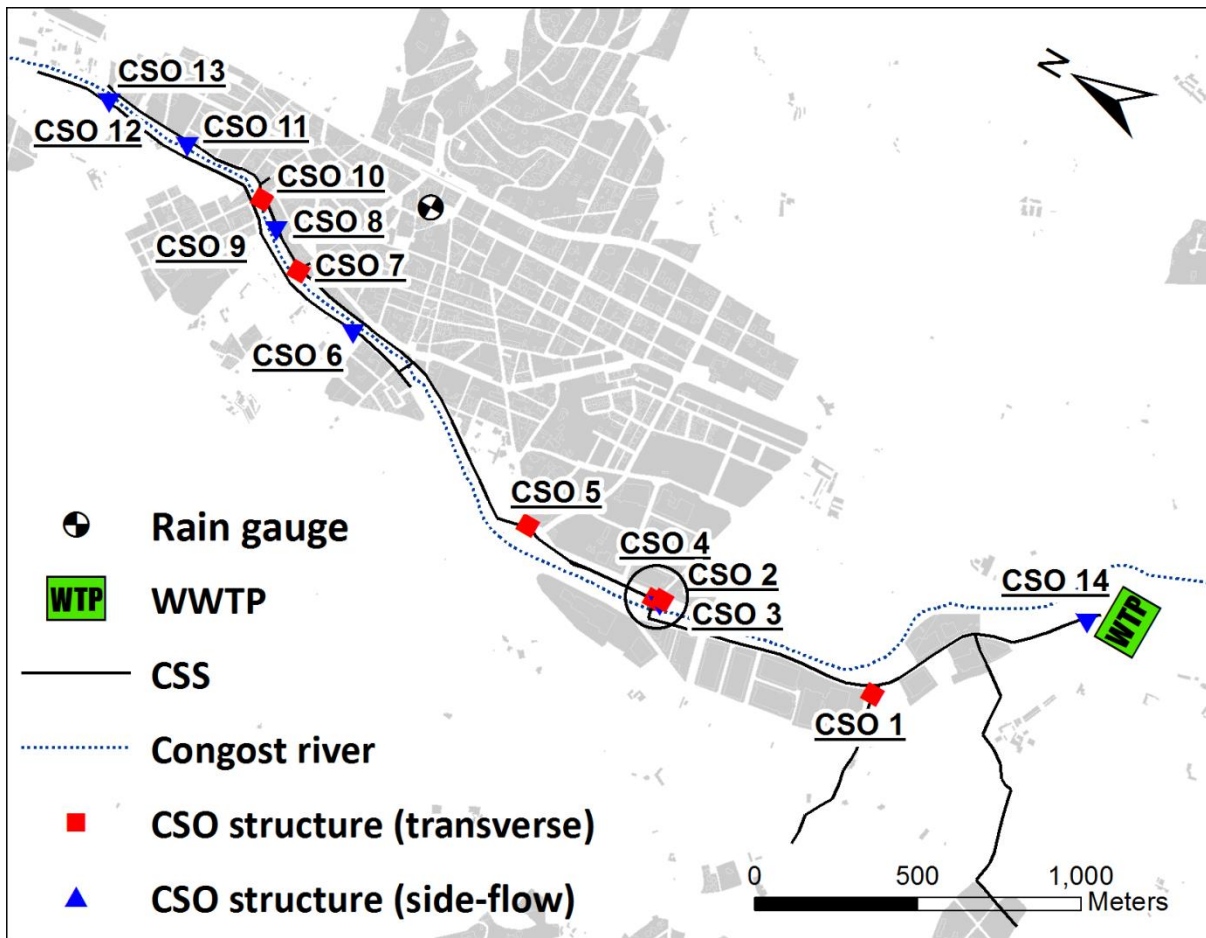
623 Tibbetts J. Combined sewer systems: Down, dirty, and out of date. *Environ Health Perspect*
624 2005;113(7):464-67.

625

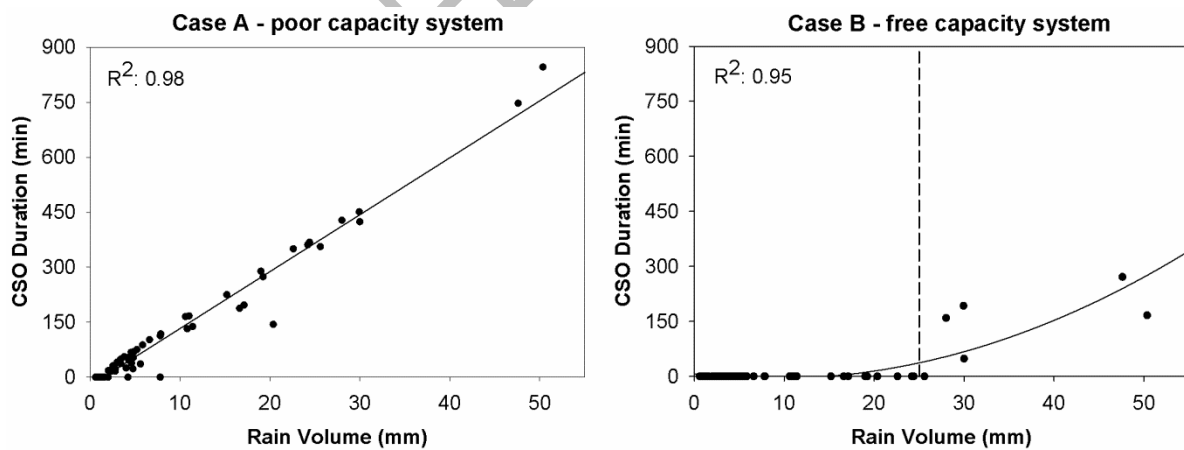
626 Zabel T, Milne I, Mckay G. Approaches adopted by the European Union and selected
627 Member States for the control of urban pollution. *Urban Water* 2001;3:25-32.

628

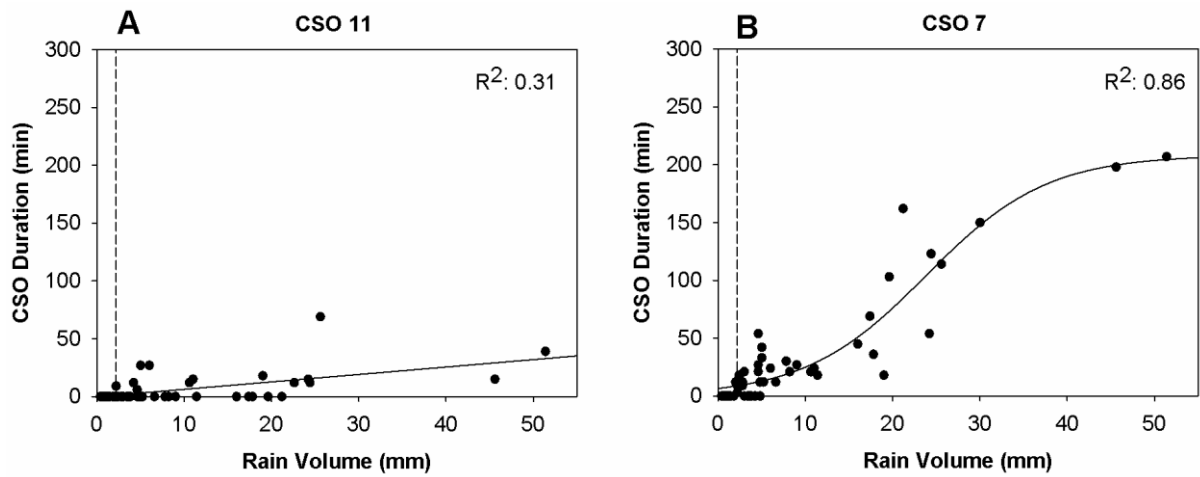
ACCEPTED MANUSCRIPT



629
 630 **Fig. 1.** Overview of the La Garriga catchment with the CSO structures numbered. The
 631 analyses were conducted using data from all of the CSO structures except Structures 9 and
 632 13.
 633

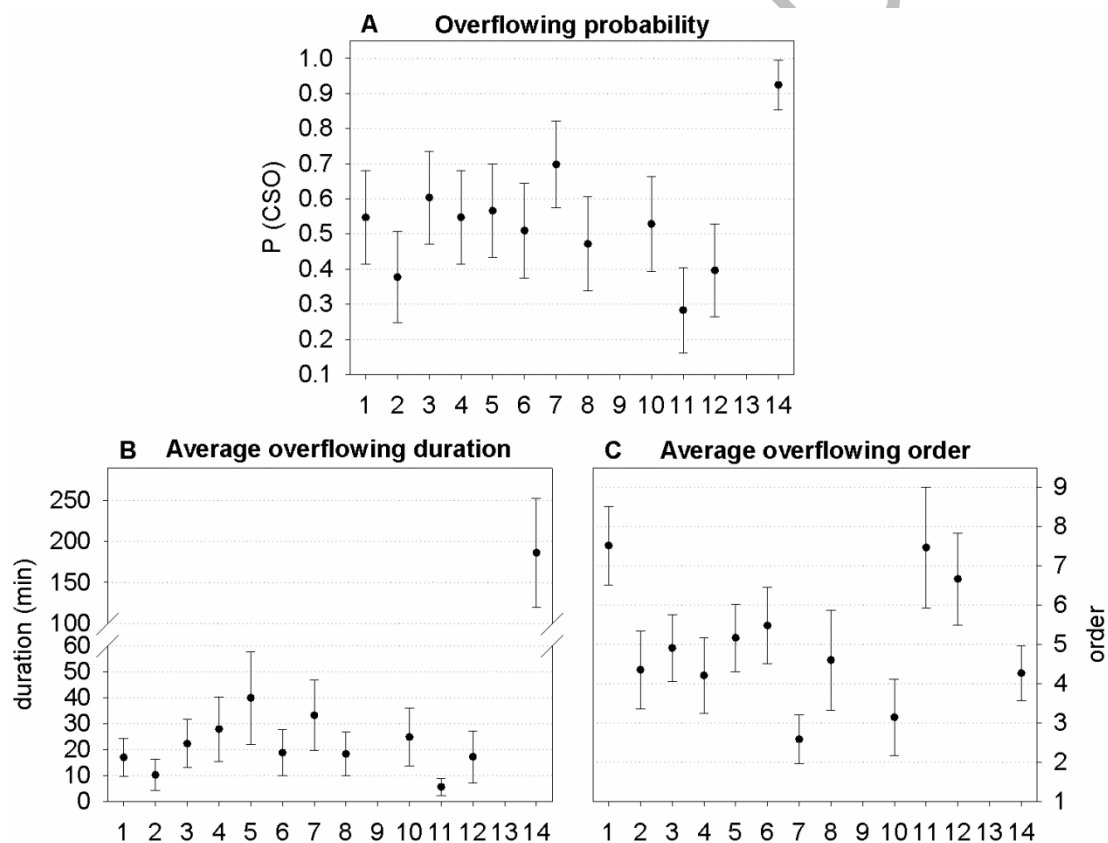


634
 635 **Fig. 2.** CSO duration versus rain volume for two hypothetical CSSs. Fig. 2A shows data from
 636 a poorly-designed CSS with high CSO activity, while Fig. 2B shows data from a system with
 637 higher capacity. In Fig. 2B, the vertical dashed line indicates approximately the maximum
 638 volume of rain (about 25 mm) that the system can assimilate before it begins to overflow.
 639
 640



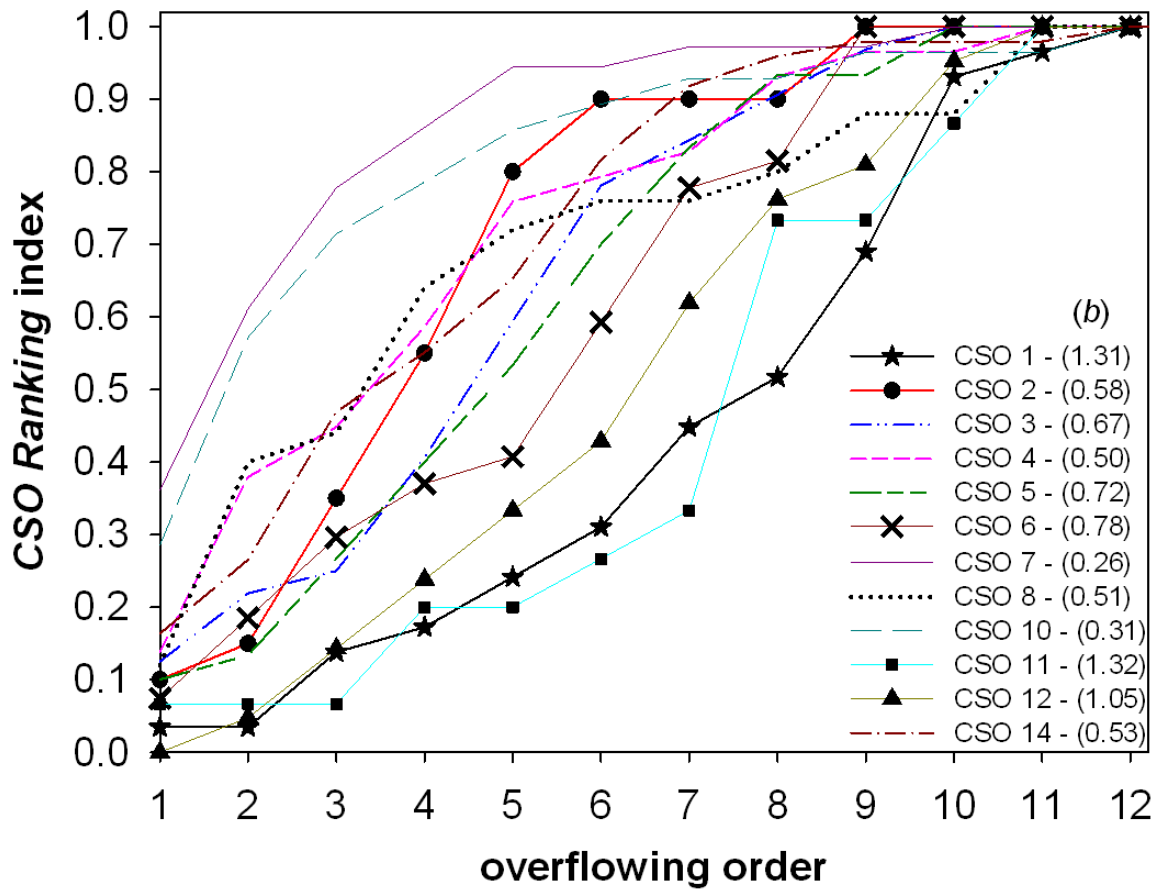
641
 642 **Fig. 3.** Rain volume versus overflow duration obtained for CSO Structures 11 and 7 during
 643 the studied period (53 rain episodes). The vertical dashed line indicates approximately the
 644 maximum rain volume that the system can assimilate before it begins to overflow, which was
 645 2.2 mm in both cases.

646
 647



648
 649 **Fig. 4.** Evaluated parameters of the CSO structures (dots represent the average value, and the
 650 lines represent the 95% *Ci*). The x-axis is each structure of the CSS (note that Structures 9
 651 and 13 do not have values because they were not used in this study).

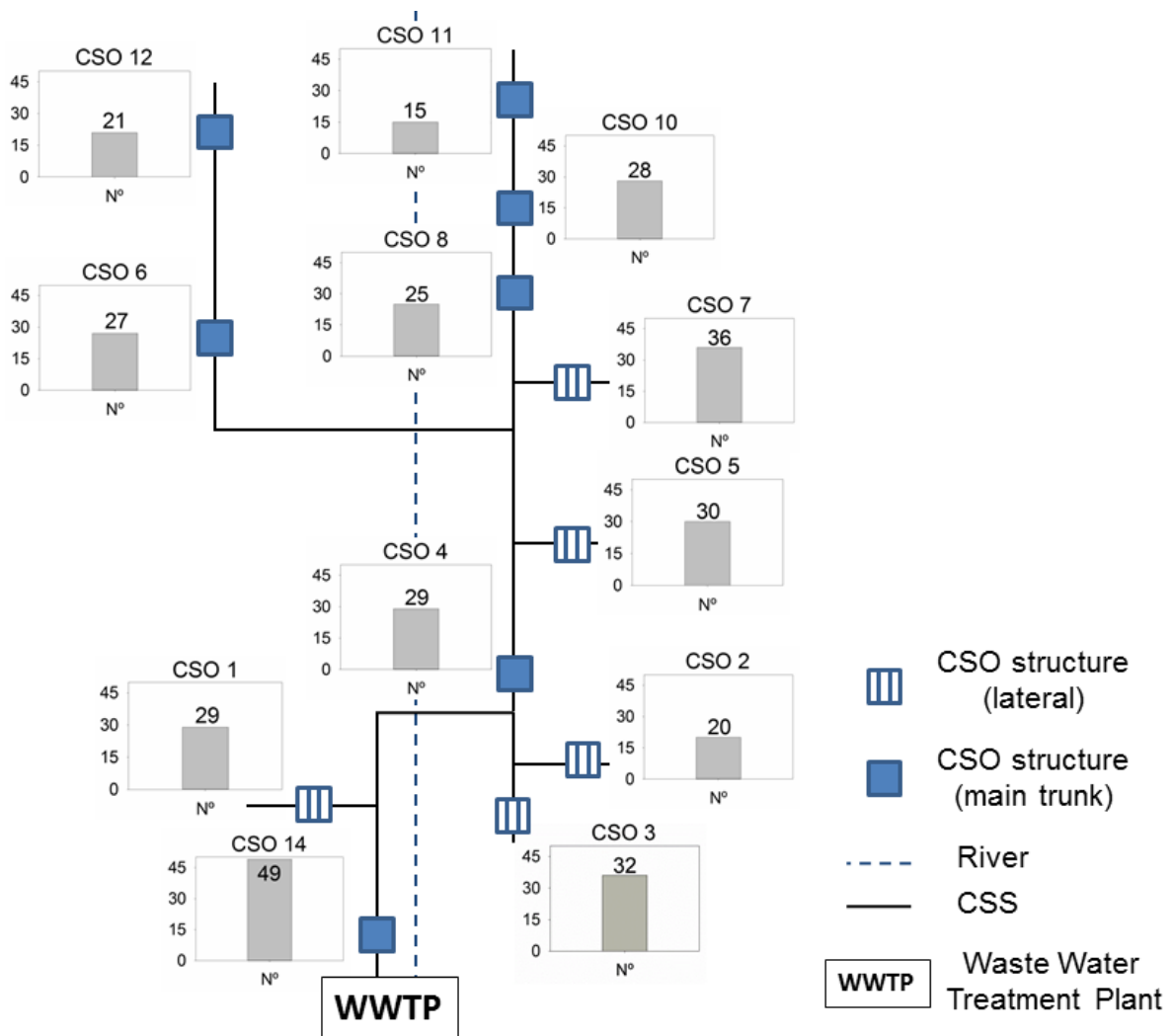
652



653
654
655
656
657

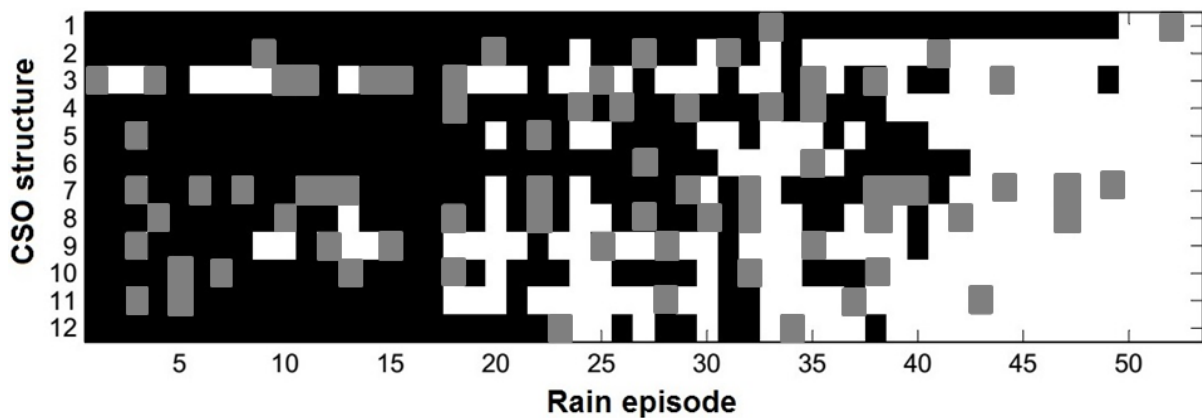
Fig. 5. Ranking curves for each CSO structure. The y-axis is the ranking index, and the x-axis is the i^{th} place of overflow in the network. In the legend shows in parentheses the value of exponent b of the power function fitted to each curve.

ACCEPTED



658
659
660
661
662

Fig. 6. Schematic of the La Garriga CSS. The number of overflows that occurred in each CSO structure during the 11-month study is graphed.



663
664
665
666
667
668
669

Fig. 7. A plot of the predicted and observed responses of each CSO structure in the La Garriga CSS for 53 rain episodes that occurred in La Garriga. The black squares indicate instances where the model correctly predicted overflow (the prediction matched observation), the white squares indicate when the model correctly predicted that an overflow did not occur, and the grey squares show where the model incorrectly predicted overflow or no overflow (the prediction did not match observation).

670
671
672
673

Table 1. Permitted number of overflows proposed by CSO regulation guidelines in different countries (adapted from De Toffol, 2006; Hernáez et al., 2011; FWR, 2012).

Country	Belgium (Flanders)	Denmark	Netherlands	USA	U.K.	Spain (Galicia)
N° CSOs per year	7	2-10	3-10	4-6	3-10	15-20

674
675
676
677

ACCEPTED MANUSCRIPT